

Article

# Analysis of the Whole-Exome Sequencing of Tumor and Circulating Tumor DNA in Metastatic Melanoma

Russell J. Diefenbach <sup>1,2</sup> , Jenny H. Lee <sup>1,2</sup>, Dario Strbenac <sup>3</sup>, Jean Y. H. Yang <sup>3,4</sup>, Alexander M. Menzies <sup>2,5,6</sup>, Matteo S. Carlino <sup>2,5,7</sup>, Georgina V. Long <sup>2,4,5,6</sup> , Andrew J. Spillane <sup>2,5,6</sup>, Jonathan R. Stretch <sup>2</sup>, Robyn P. M. Saw <sup>2,5,8</sup>, John F. Thompson <sup>2,5,8</sup>, Sydney Ch'ng <sup>2,5</sup>, Richard A. Scolyer <sup>2,4,5,9</sup> , Richard F. Kefford <sup>2,5,10</sup> and Helen Rizos <sup>1,2,\*</sup>

<sup>1</sup> Department of Biomedical Sciences, Faculty of Medicine and Health Sciences, Macquarie University, Sydney, NSW 2109, Australia; russell.diefenbach@mq.edu.au (R.J.D.); jenny.lee@mq.edu.au (J.H.L.)

<sup>2</sup> Melanoma Institute Australia, The University of Sydney, Sydney, NSW 2065, Australia; alexander.menzies@sydney.edu.au (A.M.M.); matteo.carlino@sydney.edu.au (M.S.C.); georgina.long@sydney.edu.au (G.V.L.); andrew.spillane@sydney.edu.au (A.J.S.); jonathan.stretch@melanoma.org.au (J.R.S.); robyn.saw@melanoma.org.au (R.P.M.S.); john.thompson@melanoma.org.au (J.F.T.); sydney.chng@sydney.edu.au (S.C.); richard.scolyer@health.nsw.gov.au (R.A.S.); richard.kefford@mq.edu.au (R.F.K.)

<sup>3</sup> School of Mathematics and Statistics, The University of Sydney, Sydney, NSW 2006, Australia; dario.strbenac@sydney.edu.au (D.S.); jean.yang@sydney.edu.au (J.Y.H.Y.)

<sup>4</sup> Charles Perkins Centre, The University of Sydney, Sydney, NSW 2006, Australia

<sup>5</sup> Sydney Medical School, The University of Sydney, Sydney, NSW 2006, Australia

<sup>6</sup> Department of Medical Oncology, Northern Sydney Cancer Centre, Royal North Shore Hospital, Sydney, NSW 2065, Australia

<sup>7</sup> Crown Princess Mary Cancer Centre, Westmead and Blacktown Hospitals, Sydney, NSW 2145, Australia

<sup>8</sup> Department of Melanoma and Surgical Oncology, Royal Prince Alfred Hospital, Sydney, NSW 2050, Australia

<sup>9</sup> Department of Tissue Pathology and Diagnostic Oncology, Royal Prince Alfred Hospital, Sydney, NSW 2050, Australia

<sup>10</sup> Department of Clinical Medicine, Faculty of Medicine and Health Sciences, Macquarie University, Sydney, NSW 2109, Australia

\* Correspondence: helen.rizos@mq.edu.au; Tel.: +61-298-502-762

Received: 3 October 2019; Accepted: 26 November 2019; Published: 29 November 2019



**Abstract:** The use of circulating tumor DNA (ctDNA) to monitor cancer progression and response to therapy has significant potential but there is only limited data on whether this technique can detect the presence of low frequency subclones that may ultimately confer therapy resistance. In this study, we sought to evaluate whether whole-exome sequencing (WES) of ctDNA could accurately profile the mutation landscape of metastatic melanoma. We used WES to identify variants in matched, tumor-derived genomic DNA (gDNA) and plasma-derived ctDNA isolated from a cohort of 10 metastatic cutaneous melanoma patients. WES parameters such as sequencing coverage and total sequencing reads were comparable between gDNA and ctDNA. The mutant allele frequency of common single nucleotide variants was lower in ctDNA, reflecting the lower read depth and minor fraction of ctDNA within the total circulating free DNA pool. There was also variable concordance between gDNA and ctDNA based on the total number and identity of detected variants and this was independent of the tumor biopsy site. Nevertheless, established melanoma driver mutations and several other melanoma-associated mutations were concordant between matched gDNA and ctDNA. This study highlights that WES of ctDNA could capture clinically relevant mutations present in melanoma metastases and that enhanced sequencing sensitivity will be required to identify low frequency mutations.

**Keywords:** whole exome sequencing; melanoma; circulating tumor DNA

---

## 1. Introduction

Analysis of circulating tumor DNA (ctDNA) can be used to identify therapeutically actionable mutations, monitor disease progression, detect residual disease and track the genomic evolution of treatment resistance [1–4]. The genomic profiling of ctDNA using whole genome, whole exome or targeted sequencing is feasible, but technically challenging due to the low quantities and fragmented nature of ctDNA [5–8]. Nevertheless, several reports have examined the value of sequencing patient-matched tumor gDNA and ctDNA and the results showed variable concordance in the mutation profiles of gDNA and ctDNA derived from patients with neuroblastoma, breast cancer, lung cancer or gastrointestinal malignancies [9–12]. The degree of concordance between circulating and tumor mutations appears to reflect tumor heterogeneity, which can be influenced by prior therapy, tumor stage and tumor mutation burden [12].

The NGS profiling of melanoma ctDNA and matched tumor tissue, which has been limited, is of particular interest, as tumor and ctDNA profiling has provided significant predictive and prognostic value. For instance, high tumor mutation burden predicts response, progression-free and overall survival of melanoma patients to immune checkpoint inhibitors. Longitudinal ctDNA assessment predicts progression-free survival and overall survival in stage IV melanoma patients treated with BRAF and MEK inhibitors or immunotherapy [13–15] and the melanoma-specific survival of patients with high-risk stage III resected melanoma [16]. ctDNA can also monitor the appearance of treatment-resistant melanoma subclones [14] and differentiate true progression from pseudoprogression in melanoma patients treated with immunotherapy [17]. In the majority of these studies, melanoma ctDNA and tumor tissue were evaluated separately and ctDNA analysis was limited to single mutation detection.

In this study, we examined the whole-exome sequencing (WES) mutation profiles of patient-matched melanoma tissue and matched ctDNA in a cohort of 10 patients to determine whether sequencing of these biopsies could provide complimentary, clinically actionable mutation data. We now confirm that the WES of ctDNA provides valuable mutation data, and is capable of identifying hotspot and other clinically relevant mutations, irrespective of prior therapy, timing of tissue and liquid biopsy site. However, significant enhancement of WES sensitivity is required for ctDNA to provide an accurate and complete profile of tumor subclones.

## 2. Results

### 2.1. Patient Cohort

Ten patients with metastatic melanoma with established driver BRAF or NRAS mutations were included in this study; 5/10 patients were aged 65 years or older, 8/10 were male and 6/10 had American Joint Committee on Cancer (AJCC) stage M1c disease [18] (Table 1). Time between tissue and liquid biopsy was less than 6 months in all patients (median 2.75 months, range 1–6 months), and three patients each had tissue and a liquid biopsy collected concurrently. Samples were collected prior to systemic treatment, i.e., pre-treatment (PRE) or at time of the progression of treatment (PROG). Systemic treatments included the immune checkpoint inhibitors ipilimumab, nivolumab and pembrolizumab and the targeted therapies, dabrafenib and trametinib.

**Table 1.** Patient, treatment and biopsy characteristics.

Patient	Age (Years)	Sex	Tumor Biopsy Site	Current Treatment When Tissue Biopsy Procured	Current Treatment When Liquid Biopsy Procured	Time Between Biopsies (Months) *	Mutation	Stage (AJCC 8th ed [19])	Serum LDH **	OS (Months)
1	76	M	Brain	PROG pembro	PROG pembro	Concurrent	BRAF V600E NRAS Q22K	M1d	NA	4.8
2	61	F	Inguinal LN	PROG combi-DT	PROG combi-DT	6	BRAF V600E	M1c	<ULN	Alive (33.7)
3	58	M	Brain	PRE nivo	PROG nivo	2	BRAF V600E	M1d	>2× ULN	19.2
4	48	M	Thigh SC	PROG ipi + nivo	PROG ipi + nivo	1	BRAF V600E	M1d	<ULN	20.7
5	56	M	Inguinal LN	PRE combi-DT	PROG combi-DT	4	BRAF V600K	M1c	>2× ULN	10.4
6	70	M	Liver	PRE nivo	PRE nivo	Concurrent	BRAF G466E	M1d	>2× ULN	1.2
7	37	F	Ovary	PROG ipi + pembro	PROG ipi + pembro	4	NRAS Q61K	M1c	>1× ULN	25.7
8	65	M	Abdominal LN	PROG ipi + pembro	PROG ipi + pembro	Concurrent	NRAS Q61K	M1c	<ULN	Alive (52.2)
9	65	M	Liver	PROG nivo	PROG nivo	3	NRAS Q61R	M1c	>1× ULN	20.4
10	69	M	Brain	PRE pembro	PROG pembro	6	NRAS Q61R	M1c	<ULN	11.6

\* In patients 2, 3, 4, 5 and 10, tumor biopsies were taken prior to the liquid biopsies and in patients 7 and 9, tumor biopsies were taken after the liquid biopsies. In patients 6 and 8, the liquid and tissue biopsies were taken at the same time. \*\* Taken at time of liquid biopsy. AJCC, American Joint Committee on Cancer; F, female; M, male; OS, overall survival; ULN, upper limit of normal; NA, not available; LN, lymph node; SC, subcutaneous; LN, lymph node; PRE, prior to systemic therapy; PROG, at time of progression on treatment; nivo, nivolumab (anti-PD1); pembro, pembrolizumab (anti-PD1); ipi, ipilimumab (anti-CTLA4); combi-DT, combination dabrafenib (BRAF inhibitor) and trametinib (MEK inhibitor).

## 2.2. WES and Droplet Digital PCR

The amount of tumor tissue gDNA extracted for this study was in the  $\mu\text{g}$  range and significantly higher than the ng amounts of extracted plasma ctDNA (Table S1). Nevertheless, sequencing libraries were successfully generated for ctDNA and gDNA for each patient, and WES output based on total reads and coverage was not significantly different when comparing gDNA and ctDNA (Figure 1A,B). However, the mean read depth was found to be significantly less for ctDNA, presumably due to the lower amounts of ctDNA template available for sequencing (Figure 1C). This was not always the case, however—an exception being higher ctDNA compared to gDNA mean read depth for patients 4 and 9 (Figure 1C). The coverage distributions of targeted regions by WES were also similar for gDNA and ctDNA (Figure S1).

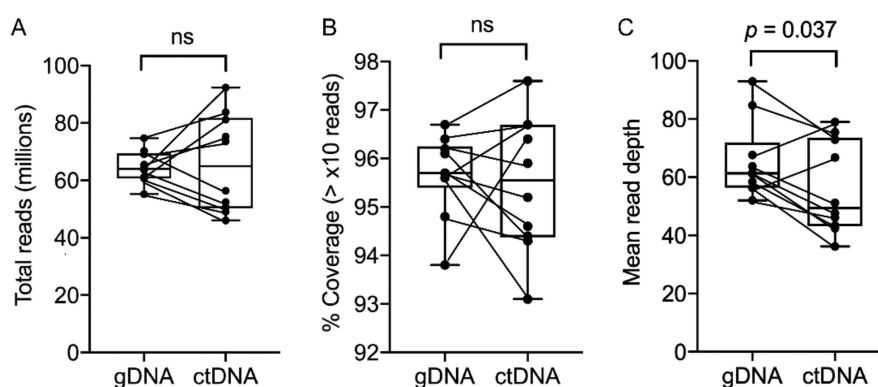


**Figure 1.** Summary of whole-exome sequencing (WES) analysis. Comparison of (A) total reads, (B) percentage of coverage ( $>10\times$  reads) and (C) mean read depth for matched (connected by lines) genomic DNA (gDNA) and circulating tumor DNA (ctDNA) from advanced melanoma patients. Plots show median with interquartile ranges and data were compared using the paired, nonparametric Wilcoxon test. Abbreviations: ns, not significant.

We also examined the relationship between ctDNA copy number and total circulating free DNA (cfDNA) quantities in the 10 melanoma patients, by measuring the amount of ctDNA using highly sensitive droplet digital (dd) PCR. We found that ctDNA copy number significantly correlated with total extracted cfDNA (Figure S2).

## 2.3. Single Nucleotide Variant Analysis

A list of single nucleotide variants (SNVs) was generated from matched gDNA and ctDNA WES. Non-synonymous SNVs with mutant allele frequency (MAF)  $\geq 10\%$  were included (summarized in Table S2). There was no significant difference in the total number of SNVs in the patient-matched tumor gDNA and ctDNA and no difference in the derived tumor mutation burden determined from WES of either gDNA or ctDNA (Figure 2).

The degree of overlap or concordance of SNVs for gDNA and ctDNA from matched patient samples ranged from 22.7% to 77.6% (Figure 3). Similar percentages of SNVs were unique to either gDNA (range 13–66.5%) or ctDNA (range 7.7–53.2%) (Figure 3). Overall, there was no detectable difference in the degree of overlap of SNVs in matched gDNA and ctDNA from individual patients regardless of treatment type (naïve, combination dabrafenib and trametinib (combi-DT) or immune checkpoint therapy), response to treatment, timing of biopsies or location of the biopsied tumor (Table 1 and Figure S3). Moreover, the three patients with concurrent tissue and liquid biopsies displayed a wide range of SNV overlap (24.5% in patient 8, 33.8% in patient 6 and 77.6% in patient 1).

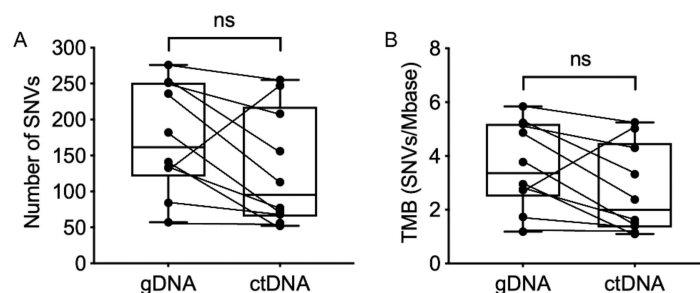


**Figure 2.** Comparison of the mutational load for melanoma patient matched (connected by lines) genomic DNA (gDNA) and circulating tumor DNA (ctDNA) analyzed by WES. **(A)** Total number of filtered single nucleotide variants (SNVs). **(B)** Tumor mutational burden (TMB). The filtered list of SNVs was produced from the WES list of total SNVs using ingenuity variant analysis, as described in Materials and Methods. The TMB was calculated as described in Materials and Methods. Plots show medians with interquartile ranges and data were compared using the paired, nonparametric Wilcoxon test. Abbreviations: ns, not significant.

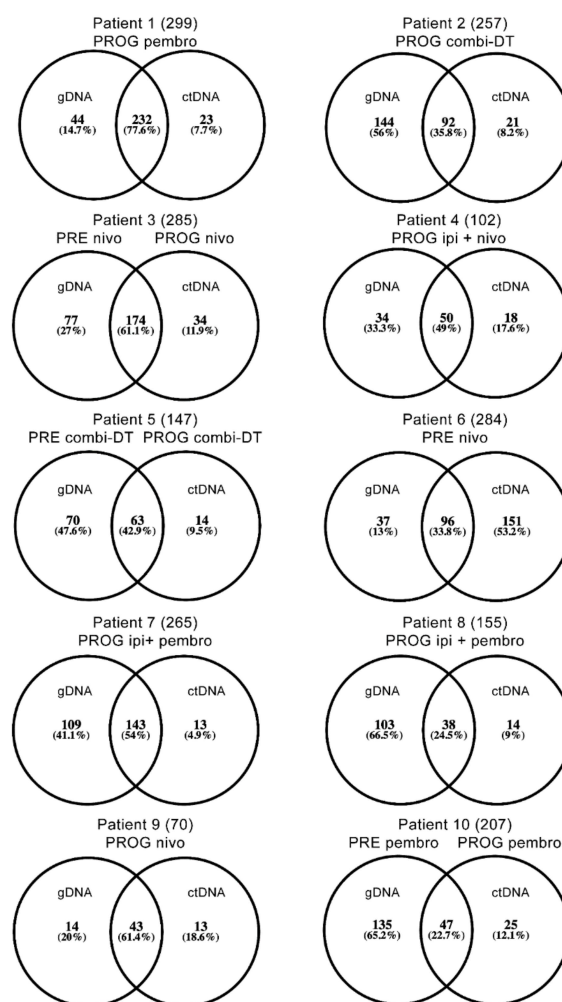


**Figure 3.** Degree of SNV overlap for patient matched genomic DNA (gDNA) and circulating tumor DNA (ctDNA) as identified by WES. The filtered list of SNVs was produced from the WES list of total SNVs using an ingenuity variant analysis as described in Materials and Methods. The numbers in parentheses represent total combined SNVs. Abbreviations: PRE, prior to systemic therapy; PROG, at time of progression of treatment; nivo, nivolumab (anti-PD1); pembro, pembrolizumab (anti-PD1); ipi, ipilimumab (anti-CTLA4); combi-DT, combination dabrafenib (BRAF inhibitor) and trametinib (MEK inhibitor).

#### 2.4. Mutant Allele Frequency (MAF) of Single Nucleotide Variants

To confirm that ctDNA sequencing provided accurate allele frequency data, we compared the MAFs for the shared SNVs in patient-matched gDNA and ctDNA. These showed significant correlations in all patients, with the highest level of correlation between gDNA and ctDNA observed in patients 6 and 9 (Figure 4 and Figure S4). Interestingly, both patients had gDNA derived from core liver biopsies (Table 1), and the high concordance between circulating and liver melanoma SNVs may reflect the fact the liver melanoma metastases tend to be larger than melanoma metastases in other sites, including brain, soft tissue and lung [20].

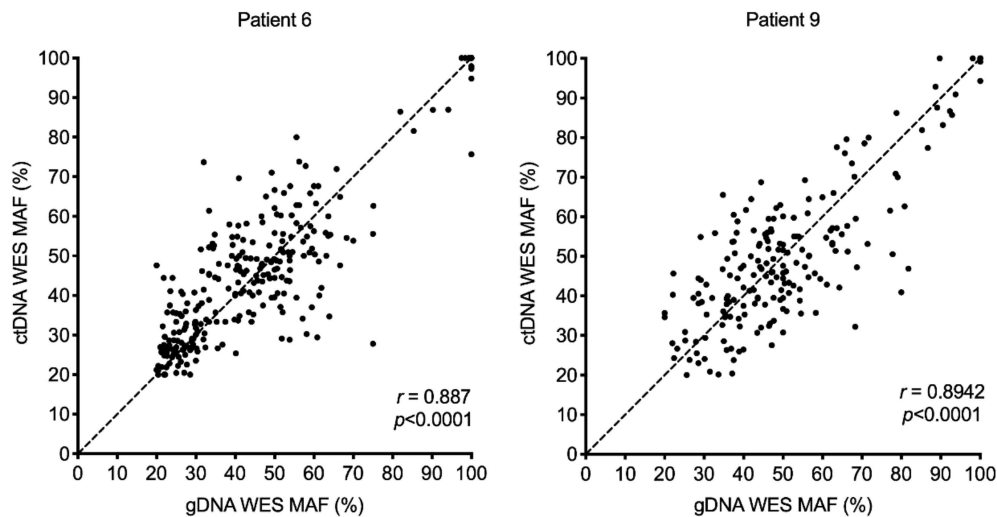


**Figure 4.** Degree of Pearson correlation between the mutant allele frequency (MAF) of SNVs common to patient-matched genomic DNA (gDNA) and circulating tumor DNA (ctDNA), as identified by WES. Dotted line indicates  $y = x$ .

#### 2.5. Melanoma Driver Mutations

We then focused on the *BRAF* and *NRAS* melanoma driver gene mutations (Table 1). WES of gDNA was able to identify the driver mutations in all patients (MAF range 25–83%), whereas WES of ctDNA only detected the driver mutation in six of ten patients (patients 1, 3, 5, 6, 7 and 9) when applying a MAF cutoff of at least 10% (with a call quality of at least 20 and read depth of at least 10 as described in Materials and Methods) (Table S3). However, the ctDNA driver mutations were detected by manual curation in the remaining four patients (patients 2, 4, 8 and 10; MAF 7–12%), and were well below the gDNA MAF (Table S3). Comparison of the driver MAF determined by WES of gDNA versus ctDNA across all 10 patients showed no significant correlation (Figure 5A). All driver MAFs in ctDNA were independently validated; nine using ddPCR analysis for either *BRAF* or *NRAS* mutations and one using highly sensitive targeted sequencing analysis (Table S3). There was significant correlation between MAF based on WES and ddPCR/targeted NGS sequencing of ctDNA (Figure 5B). However, there was less correlation (though still significant) when the driver MAF based on WES of gDNA and ddPCR analysis of ctDNA was compared (Figure 5C). This highlights that melanoma driver MAF captured in ctDNA is generally lower than the driver MAF from gDNA, consistent with our observation that MAF of common SNVs was generally lower in ctDNA WES compared to patient-matched gDNA WES data (Figure 4 and Figure S4).

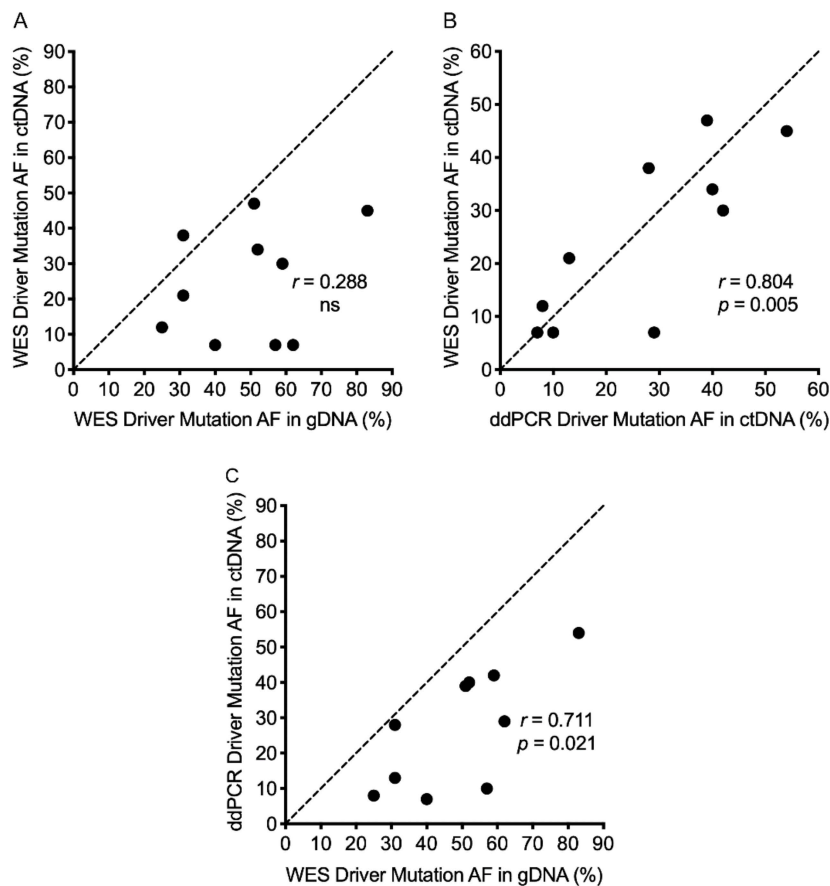


**Figure 5.** Degree of Pearson correlation based on the mutant allele frequency of the driver mutation in melanoma patients. (A) WES of genomic DNA (gDNA) versus WES of circulating tumor DNA (ctDNA). (B) ddPCR analysis of ctDNA versus WES of ctDNA. (C) WES of gDNA versus ddPCR analysis of ctDNA. Abbreviations: ns, not significant.

## 2.6. Other Highlighted Mutations

In addition to mutations in the *BRAF* or *NRAS* genes, we examined other melanoma-associated genes (gene list shown in Table S4 [21–25]) or melanoma-associated mutations (based on cBioportal [26, 27]) in the WES dataset (Table S5). These genes or mutations were detected initially in either gDNA, ctDNA or both. SNVs unique to either gDNA or ctDNA were subsequently found by manual curation of WES Bam files to occur in both sources of DNA (Table S5). Only one mutation, *MASP2* R356W, was found to be unique to ctDNA in patient 6 (Table S5). Interestingly, patient 6, the only treatment naïve patient, had the highest number of melanoma-associated mutations (Table S5), although this patient did not have the highest number of total SNVs (Figure 3). The *CDK4* R24C mutation in the *BRAF*<sup>V600E</sup> mutant patient 3 was the only additional melanoma-associated mutation predicted to be a driver mutation (Table S5). Rare germline mutations in *CDK4* at position 24 predispose to melanoma susceptibility [28]. We identified an *NRAS* Q22K mutation in patient 1 (Table S5). Although this is an uncommon *NRAS* variant, it has been reported in a small number of tumors, including melanoma [23], and potentially induces MAPK signaling [29]. It is worth noting that although this tumor was progressing on the PD1 inhibitor pembrolizumab (Table 1), this patient had progressed on prior *BRAF*/*MEK* inhibitor combination therapy, presumably due to the activating *NRAS* Q22K mutation. Inactivation mutations in *ARID2*, which encodes a component of the SWI/SNF chromatin remodeling complex, are observed in melanoma [23], and the nonsense *ARID* Q1165\* mutation was enriched in the ctDNA of patient 8 (Table S5). The *MAP3K5* R256C mutation identified in ctDNA and melanoma

gDNA from patient 10 has also been identified in melanoma, and shown to inhibit the pro-death activity of this kinase [30].

### 3. Discussion

In this study we compared the WES of matched gDNA and ctDNA from 10 patients with metastatic melanoma in both treatment naïve patients and patients on systemic molecular or immune therapies. We now report that ctDNA sequencing provides an accurate, albeit incomplete snapshot of the mutation profile and mutation burden of the patient-matched metastatic tumor. The SNVs found in the patient-matched melanoma gDNA and ctDNA overlapped by 22.7% to 77.6%, which is comparable to gDNA and ctDNA mutation concordance data reported for other cancers [9,10,12,31]. A major caveat of this work is the lack of patient-matched germline analyses, and although we applied a stringent bioinformatic filtering approach to enrich for somatic variants, the number of somatic variants and the concordance data may have been overestimated. Nevertheless, the ctDNA mutation profiling provided a valuable mutation profile irrespective of the site of the patient-matched tumor and this was particularly important for brain metastases, given that levels of ctDNA derived from brain metastases are extremely low, possibly as a result of the blood–brain barrier [15,32]. It is likely that ctDNA in these melanoma patients is derived from extracranial tumors, and ctDNA remains informative for brain melanoma because melanoma brain tumors have similar mutational and treatment response profiles to concurrent extracranial tumors [33–37]. It is also worth noting that MAFs of common SNVs were most concordant between ctDNA and liver melanoma metastases.

One recent study found substantial discordance between NGS of matched gDNA and ctDNA in several tumor types (including one melanoma sample) and reported that ctDNA analysis may improve detection of hotspot and actionable mutations compared to gDNA alone [12]. Tissue and circulating DNA mutation concordance was reported to be higher in patients who had received systemic therapy and in cancers with high TMB [12]. In our study, 9/10 patients received some sort of systemic treatment, and although melanoma has a very high TMB [38], the concordance between gDNA and ctDNA mutations was variable. Furthermore, although our cohort consisted of gDNA and ctDNA samples collected at different time points, the timing of sample collection was not associated with mutation concordance in our report and in another similar study [12].

The majority of SNVs detected in our study, including the *BRAF* and *NRAS* driver mutations, showed lower MAFs in ctDNA compared to gDNA, and this was presumably due to the combination of lower read depth for ctDNA and the fact that ctDNA makes up only a fraction of total cfDNA [39]. For a few variants, however, including *NRAS* Q22K and *CDK4* R24C, and the MAFs in ctDNA, were higher or equivalent to the MAFs in tumor tissue, suggesting the subclonal expression of these mutations in the lesion sequenced. We also applied a MAF threshold of at least 10% to define variants in the gDNA and ctDNA sequencing data. In some samples, a lower MAF threshold was required to detect the *BRAF* and *NRAS* driver mutations and allele frequency thresholds need to be optimized for sensitivity and specificity with larger cohort studies. Although ddPCR analysis of ctDNA was more sensitive than WES ctDNA sequencing, the additional information gained by unbiased sequencing, including tumor mutation burden, which is associated with clinical benefit for immunotherapy [31] and the potential to define resistant subclones, is an important advantage. For instance, we identified an activating and putative resistance *NRAS* mutation (Q22K) in both gDNA and ctDNA in a *BRAF*-mutant melanoma after progression on combined *BRAF* and *MEK* inhibitors [40]. There is also significant scope to improve the sensitivity of ctDNA sequencing with multi-gene panels, molecular barcoding and size selection enrichment.

In conclusion, WES analysis of total SNVs in ctDNA provides a valuable snapshot of the mutational landscape and burden of melanoma metastases, although additional improvements in sensitivity are required, especially for the analysis of smaller-sized descendent tumor subclones. This may be clinically important as pre-existing variants capable of promoting treatment resistance may cause a fitness deficit and produce only minor descendent clones in the absence of selective pressure. This

appears to be the case, for instance, for BRAF V600E gene amplification, a common mediator of resistance to BRAF and MEK inhibitors [41], which also promotes proliferative arrest in the absence of MAPK inhibitors. Thus, the use of ctDNA to identify the tumor metagenome (i.e., the aggregate of co-existent tumor subclones) will require sequencing depth that allows the detection of 0.1% MAF afforded by targeted gene panels [42,43]. At this MAF threshold, ctDNA is detectable in 75% of metastatic melanoma patients [13], and improving the sensitivity of ctDNA sequencing promises significant benefits, especially as a predictive biomarker in an era with many effective therapies.

## 4. Materials and Methods

### 4.1. Human Melanoma Samples

The fresh-frozen tissue and blood samples used in the current study were obtained from the Melanoma Institute Australia biospecimen bank with written informed patient consent and institutional review board approval (Sydney Local Health District Human Research Ethics Committee, Protocol Numbers X15–0454 and HREC/11/RPAH/444). All samples were pathologically assessed prior to inclusion into the study, as previously described [44].

Blood (10 mL) was collected in EDTA tubes (Becton Dickinson, Franklin Lakes, NJ, USA) and processed immediately. Tubes were spun at  $800\times g$  for 15 min at room temperature. Plasma was then removed into new 15 mL tubes without disturbing the buffy coat and respun at  $1600\times g$  for 10 min at room temperature to remove cellular debris. Plasma was stored in 1 mL aliquots at  $-80^{\circ}\text{C}$ .

### 4.2. DNA Extractions

Tumor-derived gDNA for WES was extracted from fresh-frozen tissue using the DNeasy Blood and Tissue Kit (Qiagen, Hilden, Germany) according to the manufacturer's instructions. Plasma ctDNA from melanoma patients was purified using the QIAamp circulating nucleic acid kit (Qiagen, Hilden, Germany) according to the manufacturer's instructions. ctDNA was purified from 3–5 mL of plasma, and the final elution volume was 30–40  $\mu\text{L}$ .

### 4.3. Analysis of Purified ctDNA from Plasma

The copy number of ctDNA extracted from plasma was analyzed as previously described [15]. The QX200 ddPCR system was used to detect mutant *NRAS* or *BRAF* as previously described (Bio-Rad, Hercules, CA, USA) [15]. The copy number was determined with Quantasoft software version 1.7.4 (Bio-Rad, Hercules, CA, USA) using a manual threshold setting. One patient ctDNA sample was analyzed by ThermoFisher Scientific Australia using their lung oncomine cfDNA assay according to the manufacturer's instructions.

### 4.4. Whole Exome Sequencing

Exome library preparation and sequencing workflow utilized the SureSelect V5-post capture kit (Agilent, Santa Clara, CA, USA) and Illumina (San Diego, CA, USA) HiSeq 4000 platform and was performed by the Macrogen corporation (Seoul, South Korea). Total DNA was quantified using a Quant-iT Picogreen dsDNA assay kit (Life Technologies, Carlsbad, CA, USA). The size of sequencing library preparations was ascertained on a 2100 Bioanalyzer (Agilent, Santa Clara, CA, USA) using a DNA 1000 chip. The quantity of individual sequencing libraries was determined using qPCR quantification (Illumina, San Diego, CA, USA) according to the manufacturer's instructions. Sequencing reads were mapped using Burrows-Wheeler Aligner (BWA) [45] against the human reference genome hg19 (<https://genome.ucsc.edu>). SNPs were detected using SAMTools [46], variant database dbSNP [47] and 1000 genomes project [48]. Whole exome sequence data have been deposited in the Sequence Read Archive database, Accession PRJNA592419.

#### 4.5. Filtered Single Nucleotide Variants

Filtered SNV annotation and interpretation analyses were generated through the use of Ingenuity Variant Analysis software (<https://www.qiagenbioinformatics.com/product-login/>) from Qiagen (Hilden, Germany).

Since no matched normal tissue or germline DNA was available, we applied a stringent mutation filtering pipeline based on a recently validated somatic mutation filtering strategy [49]. Included SNVs were those with a call quality of at least 20, a read depth of at least 10 and allele-frequency of at least 10. Included SNVs were exonic or the first 2 bases of introns flanking exons, and were classified as disease-associated according to the human gene mutation database (HGMD) or ClinVar or established gain of function or frameshift, indels, or stop-codon or missense mutation unless predicted to be innocuous by SIFT or Polyphen. Included SNVs were also those outside the top 5.0% most exonically variable 100 base windows in healthy public genomes (1000 genomes project) and outside the top 1% most exonically variable genes in the 1000 genomes project [48]). Excluded SNVs that were likely to be polymorphisms were those observed with an allele frequency greater than or equal to 1.0% of the genomes in the 1000 genomes project [48], NHLBI ESP exomes [50], the ExAC dataset [51] or gnomAD [51]. Excluded SNVs included those present in at least 20% of the gDNA or ctDNA patient samples (excluding driver mutations) that are experimentally observed to be associated with a possibly benign phenotype. Further manual filtering consisted of including only exonic SNVs that were non-synonymous mutations and excluding any SNVs still present in the 1000 genomes project.

Melanoma-associated genes were identified using several sources [21–25]. Melanoma-associated mutations were confirmed using cBioportal [26,27] (<http://www.cbioportal.org>). The tumor mutational burden (SNVs/Mbase) was calculated using a human exome size (Mbase) based on the number of on-target genotypes (with more than 10× sequencing depth) determined for each patient sample subjected to WES and the total number of filtered SNVs.

#### 4.6. Statistical Analysis

Venn diagrams were generated using the interactive online tool Venny 2.1 <http://bioinfogp.cnb.csic.es/tools/venny/index.html>. Pearson correlation coefficients were determined using Prism version 8.1.1. A paired, nonparametric Wilcoxon test was also performed using Prism.

### 5. Conclusions

In this study, we showed that sequencing of ctDNA to capture the mutational profiles and mutation burdens of melanoma metastases is a viable option. The sequencing read depth of ctDNA was consistently lower than gDNA, and thus mutation detection sensitivity is an important limitation, particularly in patients with low tumor burden or intracranial disease. Although WES was used in the current study, this approach is likely to be superseded by targeted deep sequencing due its greater sensitivity accomplished through greater read depth. This is certainly feasible for melanoma, where a targeted gene panel can be designed to cover the majority of known somatic mutations.

**Supplementary Materials:** The following are available online at <http://www.mdpi.com/2072-6694/11/12/1905/s1>. Figure S1: Histograms of reading depth distribution in target regions covered by WES for patient matched gDNA and ctDNA, Figure S2: Pearson correlation of total plasma cfDNA extracted from melanoma patients with copy number of ctDNA determined by ddPCR, Figure S3: Comparison of time between biopsies of patient matched genomic DNA and circulating tumor DNA versus concordance (% overlap of SNVs from WES), Figure S4: Degree of Pearson correlation between the MAF of SNVs common to patient matched gDNA and ctDNA as identified by WES, Table S1: DNA quantity, Table S2: Filtered SNVs, Table S3: Driver melanoma mutations, Table S4: Melanoma genes, Table S5: Highlighted melanoma-associated mutations.

**Author Contributions:** Conceptualization, R.J.D., J.H.L. and H.R.; methodology, R.J.D., J.H.L. and H.R.; formal analysis, R.J.D., J.H.L., D.S., J.Y.H.Y. and H.R.; investigation, R.J.D. and J.H.L.; resources, R.F.K., A.M.M., M.S.C., G.V.L., A.J.S., J.R.S., R.P.M.S., J.F.T., S.C. and R.A.S.; writing—original draft preparation, R.J.D. and H.R.; writing—review and editing, R.J.D., J.H.L., D.S., J.Y.H.Y., R.F.K., A.M.M., M.S.C., G.V.L., A.J.S., J.R.S., R.P.M.S., J.F.T., S.C., R.A.S. and H.R.; visualization, R.J.D., J.H.L. and H.R.; supervision, H.R.; project administration, H.R.; funding acquisition, H.R.

**Funding:** R.J.D. was supported in part by a donation to Melanoma Institute Australia from the Clearbridge Foundation. This work was also supported in part by the National Health and Medical Research Council (APP1093017 and APP1128951). H.R., R.A.S. and G.V.L. are supported by National Health and Medical Research Council Research Fellowships (APP1104503, APP1141295 and APP1119059). G.V.L. and J.F.T. are also supported by the Medical Foundation of the University of Sydney. A.M.M. is supported by a Cancer Institute NSW Fellowship. J.R.S. and R.P.M.S. are supported by Melanoma Institute Australia. Support from colleagues at Melanoma Institute Australia, the Royal Prince Alfred Hospital and Westmead Hospital is also gratefully acknowledged.

**Conflicts of Interest:** G.V.L. receives consultant service fees from Amgen, BMS, Array, Pierre-Fabre, Novartis, Merck Sharp and Dohme (MSD) and Roche. A.M.M. is an advisory board member for BMS, MSD, Novartis, Roche and Pierre Fabre. R.F.K. has been on advisory boards for Roche, Amgen, BMS, MSD, Novartis and TEVA and has received honoraria from MSD, BMS and Novartis. M.S.C. is an advisory board member for MSD, BMS, Novartis, Pierre-Fabre, Roche and Amgen. R.A.S. has received honoraria from MSD, Novartis, GSK, BMS, Myriad and NeraCare. J.F.T. has been on advisory boards for GlaxoSmithKline, Provectus Inc, Merck Sharp Dohme and Bristol Myers Squibb, and has received honoraria and travel support from GlaxoSmithKline and Provectus Inc. He has received honoraria for advisory board participation from Merck Sharp Dohme and Bristol Myers Squibb. These companies had no role in the design of the study; in the collection, analyses, or interpretation of data; in the writing of the manuscript, or in the decision to publish the results. All remaining authors have declared no conflicts of interest.

## References

1. Yi, X.; Ma, J.; Guan, Y.; Chen, R.; Yang, L.; Xia, X. The feasibility of using mutation detection in ctDNA to assess tumor dynamics. *Int. J. Cancer* **2017**, *140*, 2642–2647. [[CrossRef](#)] [[PubMed](#)]
2. Wan, J.C.M.; Massie, C.; Garcia-Corbacho, J.; Mouliere, F.; Brenton, J.D.; Caldas, C.; Pacey, S.; Baird, R.; Rosenfeld, N. Liquid biopsies come of age: Towards implementation of circulating tumour DNA. *Nat. Rev. Cancer* **2017**, *17*, 223–238. [[CrossRef](#)] [[PubMed](#)]
3. De Rubis, G.; Krishnan, S.R.; Bebawy, M. Circulating tumor DNA—Current state of play and future perspectives. *Pharmacol. Res.* **2018**, *136*, 35–44. [[CrossRef](#)] [[PubMed](#)]
4. Donaldson, J.; Park, B.H. Circulating tumor DNA: Measurement and clinical utility. *Annu. Rev. Med.* **2018**, *69*, 223–234. [[CrossRef](#)] [[PubMed](#)]
5. Klevebring, D.; Neiman, M.; Sundling, S.; Eriksson, L.; Darai Ramqvist, E.; Celebioglu, F.; Czene, K.; Hall, P.; Egevad, L.; Gronberg, H.; et al. Evaluation of exome sequencing to estimate tumor burden in plasma. *PLoS ONE* **2014**, *9*, e104417. [[CrossRef](#)]
6. Ahlborn, L.B.; Rohrberg, K.S.; Gabrielaite, M.; Tuxen, I.V.; Yde, C.W.; Spanggaard, I.; Santoni-Rugiu, E.; Nielsen, F.C.; Lassen, U.; Mau-Sorensen, M.; et al. Application of cell-free DNA for genomic tumor profiling: A feasibility study. *Oncotarget* **2019**, *10*, 1388–1398. [[CrossRef](#)]
7. Butler, T.M.; Johnson-Camacho, K.; Peto, M.; Wang, N.J.; Macey, T.A.; Korkola, J.E.; Koppie, T.M.; Corless, C.L.; Gray, J.W.; Spellman, P.T. Exome sequencing of cell-free DNA from metastatic cancer patients identifies clinically actionable mutations distinct from primary disease. *PLoS ONE* **2015**, *10*, e0136407. [[CrossRef](#)]
8. Murtaza, M.; Dawson, S.J.; Tsui, D.W.; Gale, D.; Forshew, T.; Piskorz, A.M.; Parkinson, C.; Chin, S.F.; Kingsbury, Z.; Wong, A.S.; et al. Non-invasive analysis of acquired resistance to cancer therapy by sequencing of plasma DNA. *Nature* **2013**, *497*, 108–112. [[CrossRef](#)]
9. Chicard, M.; Colmet-Daage, L.; Clement, N.; Danzon, A.; Bohec, M.; Bernard, V.; Baulande, S.; Bellini, A.; Deveau, P.; Pierron, G.; et al. Whole-exome sequencing of cell-free DNA reveals temporo-spatial heterogeneity and identifies treatment-resistant clones in neuroblastoma. *Clin. Cancer Res.* **2018**, *24*, 939–949. [[CrossRef](#)]
10. Dietz, S.; Schirmer, U.; Merce, C.; von Bubnoff, N.; Dahl, E.; Meister, M.; Muley, T.; Thomas, M.; Sultmann, H. Low input whole-exome sequencing to determine the representation of the tumor exome in circulating DNA of non-small cell lung cancer patients. *PLoS ONE* **2016**, *11*, e0161012. [[CrossRef](#)]
11. Jimenez, I.; Chicard, M.; Colmet-Daage, L.; Clement, N.; Danzon, A.; Lapouble, E.; Pierron, G.; Bohec, M.; Baulande, S.; Berrebi, D.; et al. Circulating tumor DNA analysis enables molecular characterization of pediatric renal tumors at diagnosis. *Int. J. Cancer* **2018**, *144*, 68–79. [[CrossRef](#)] [[PubMed](#)]
12. Imperial, R.; Nazer, M.; Ahmed, Z.; Kam, A.E.; Pluard, T.J.; Bahaj, W.; Levy, M.; Kuzel, T.M.; Hayden, D.M.; Pappas, S.G.; et al. Matched whole-genome sequencing (WGS) and whole-exome sequencing (WES) of tumor tissue with circulating tumor DNA (ctDNA) analysis: Complementary modalities in clinical practice. *Cancers* **2019**, *11*, 1399. [[CrossRef](#)] [[PubMed](#)]

13. Santiago-Walker, A.; Gagnon, R.; Mazumdar, J.; Casey, M.; Long, G.V.; Schadendorf, D.; Flaherty, K.; Kefford, R.; Hauschild, A.; Hwu, P.; et al. Correlation of BRAF mutation status in circulating-free DNA and tumor and association with clinical outcome across four BRAFi and MEKi clinical trials. *Clin. Cancer Res.* **2016**, *22*, 567–574. [[CrossRef](#)] [[PubMed](#)]
14. Gray, E.S.; Rizos, H.; Reid, A.L.; Boyd, S.C.; Pereira, M.R.; Lo, J.; Tembe, V.; Freeman, J.; Lee, J.H.; Scolyer, R.A.; et al. Circulating tumor DNA to monitor treatment response and detect acquired resistance in patients with metastatic melanoma. *Oncotarget* **2015**, *6*, 42008–42018. [[CrossRef](#)]
15. Lee, J.H.; Long, G.V.; Boyd, S.; Lo, S.; Menzies, A.M.; Tembe, V.; Guminski, A.; Jakrot, V.; Scolyer, R.A.; Mann, G.J.; et al. Circulating tumour DNA predicts response to anti-PD1 antibodies in metastatic melanoma. *Ann. Oncol.* **2017**, *28*, 1130–1136. [[CrossRef](#)]
16. Lee, J.H.; Saw, R.P.; Thompson, J.F.; Lo, S.; Spillane, A.J.; Shannon, K.F.; Stretch, J.R.; Howle, J.; Menzies, A.M.; Carlino, M.S.; et al. Pre-operative ctDNA predicts survival in high-risk stage III cutaneous melanoma patients. *Ann. Oncol.* **2019**, *30*, 815–822. [[CrossRef](#)]
17. Lee, J.H.; Long, G.V.; Menzies, A.M.; Lo, S.; Guminski, A.; Whitbourne, K.; Peranec, M.; Scolyer, R.; Kefford, R.F.; Rizos, H.; et al. Association between circulating tumor DNA and pseudoprogression in patients with metastatic melanoma treated with anti-programmed cell death 1 antibodies. *JAMA Oncol.* **2018**, *4*, 717–721. [[CrossRef](#)]
18. Gershenwald, J.E.; Scolyer, R.A.; Hess, K.R.; Sondak, V.K.; Long, G.V.; Ross, M.I.; Lazar, A.J.; Faries, M.B.; Kirkwood, J.M.; McArthur, G.A.; et al. Melanoma staging: Evidence-based changes in the American Joint Committee on Cancer eighth edition cancer staging manual. *CA Cancer J. Clin.* **2017**, *67*, 472–492. [[CrossRef](#)]
19. Gershenwald, J.E.; Scolyer, R.A.; Hess, K.R.; Thompson, J.F.; Long, G.V.; Ross, M.I. Melanoma of the skin. In *AJCC Cancer Staging Manual*; Amin, M.B., Edge, S., Greene, F., Byrd, D.R., Brookland, R.K., Washington, M.K., Gershenwald, J.E., Compton, C.C., Hess, K.R., Sullivan, D.C., et al., Eds.; Springer: New York, NY, USA, 2017; pp. 563–585.
20. Pires da Silva, I.; Lo, S.; Quek, C.; Gonzalez, M.; Carlino, M.S.; Long, G.V.; Menzies, A.M. Site-specific response patterns, pseudoprogression, and acquired resistance in patients with melanoma treated with ipilimumab combined with anti-PD-1 therapy. *Cancer* **2019**. [[CrossRef](#)]
21. The Cancer Genome Atlas Network. Genomic classification of cutaneous melanoma. *Cell* **2015**, *161*, 1681–1696. [[CrossRef](#)]
22. Robertson, A.G.; Shih, J.; Yau, C.; Gibb, E.A.; Oba, J.; Mungall, K.L.; Hess, J.M.; Uzunangelov, V.; Walter, V.; Danilova, L.; et al. Integrative analysis identifies four molecular and clinical subsets in uveal melanoma. *Cancer Cell* **2017**, *32*, 204–220.e15. [[CrossRef](#)] [[PubMed](#)]
23. Hodis, E.; Watson, I.R.; Kryukov, G.V.; Arold, S.T.; Imielinski, M.; Theurillat, J.P.; Nickerson, E.; Auclair, D.; Li, L.; Place, C.; et al. A landscape of driver mutations in melanoma. *Cell* **2012**, *150*, 251–263. [[CrossRef](#)] [[PubMed](#)]
24. Arafah, R.; Qutob, N.; Emmanuel, R.; Keren-Paz, A.; Madore, J.; Elkahloun, A.; Wilmott, J.S.; Gartner, J.J.; Di Pizio, A.; Winograd-Katz, S.; et al. Recurrent inactivating RASA2 mutations in melanoma. *Nat. Genet.* **2015**, *47*, 1408–1410. [[CrossRef](#)] [[PubMed](#)]
25. Newell, F.; Kong, Y.; Wilmott, J.S.; Johansson, P.A.; Ferguson, P.M.; Cui, C.; Li, Z.; Kazakoff, S.H.; Burke, H.; Dodds, T.J.; et al. Whole-genome landscape of mucosal melanoma reveals diverse drivers and therapeutic targets. *Nat. Commun.* **2019**, *10*, 3163. [[CrossRef](#)] [[PubMed](#)]
26. Gao, J.; Aksoy, B.A.; Dogrusoz, U.; Dresdner, G.; Gross, B.; Sumer, S.O.; Sun, Y.; Jacobsen, A.; Sinha, R.; Larsson, E.; et al. Integrative analysis of complex cancer genomics and clinical profiles using the cBioPortal. *Sci. Signal.* **2013**, *6*, p11. [[CrossRef](#)] [[PubMed](#)]
27. Cerami, E.; Gao, J.; Dogrusoz, U.; Gross, B.E.; Sumer, S.O.; Aksoy, B.A.; Jacobsen, A.; Byrne, C.J.; Heuer, M.L.; Larsson, E.; et al. The cBio cancer genomics portal: An open platform for exploring multidimensional cancer genomics data. *Cancer Discov.* **2012**, *2*, 401–404. [[CrossRef](#)]
28. Puntervoll, H.E.; Yang, X.R.; Vetti, H.H.; Bachmann, I.M.; Avril, M.F.; Benfodda, M.; Catricala, C.; Dalle, S.; Duval-Modeste, A.B.; Ghorzo, P.; et al. Melanoma prone families with CDK4 germline mutation: Phenotypic profile and associations with MC1R variants. *J. Med. Genet.* **2013**, *50*, 264–270. [[CrossRef](#)]
29. Loree, J.M.; Miron, B.; Holla, V.; Overman, M.J.; Pereira, A.A.L.; Lam, M.; Morris, V.K.; Raghav, K.P.S.; Routbort, M.; Shaw, K.R.; et al. Not all RAS mutations created equal: Functional and clinical characterization of 80 different KRAS and NRAS mutations. *J. Clin. Oncol.* **2017**, *35*, 3589. [[CrossRef](#)]

30. Prickett, T.D.; Zerlanko, B.; Gartner, J.J.; Parker, S.C.J.; Dutton-Regester, K.; Lin, J.C.; Teer, J.K.; Wei, X.; Jiang, J.; Nisc Comparative Sequencing, P.; et al. Somatic mutations in MAP3K5 attenuate its proapoptotic function in melanoma through increased binding to thioredoxin. *J. Invest. Dermatol.* **2014**, *134*, 452–460. [[CrossRef](#)]
31. Koepfel, F.; Blanchard, S.; Jovelet, C.; Genin, B.; Marcaillou, C.; Martin, E.; Rouleau, E.; Solary, E.; Soria, J.C.; Andre, F.; et al. Whole exome sequencing for determination of tumor mutation load in liquid biopsy from advanced cancer patients. *PLoS ONE* **2017**, *12*, e0188174. [[CrossRef](#)]
32. De Mattos-Arruda, L.; Mayor, R.; Ng, C.K.Y.; Weigelt, B.; Martinez-Ricarte, F.; Torrejon, D.; Oliveira, M.; Arias, A.; Raventos, C.; Tang, J.; et al. Cerebrospinal fluid-derived circulating tumour DNA better represents the genomic alterations of brain tumours than plasma. *Nat. Commun.* **2015**, *6*, 8839. [[CrossRef](#)] [[PubMed](#)]
33. Fischer, G.M.; Jalali, A.; Kircher, D.A.; Lee, W.C.; McQuade, J.L.; Haydu, L.E.; Joon, A.Y.; Reuben, A.; de Macedo, M.P.; Carapeto, F.C.L.; et al. Molecular profiling reveals unique immune and metabolic features of melanoma brain metastases. *Cancer Discov.* **2019**, *9*, 628–645. [[CrossRef](#)] [[PubMed](#)]
34. Long, G.V.; Atkinson, V.; Lo, S.; Sandhu, S.; Guminski, A.D.; Brown, M.P.; Wilmott, J.S.; Edwards, J.; Gonzalez, M.; Scolyer, R.A.; et al. Combination nivolumab and ipilimumab or nivolumab alone in melanoma brain metastases: A multicentre randomised phase 2 study. *Lancet Oncol.* **2018**, *19*, 672–681. [[CrossRef](#)]
35. Davies, M.A.; Saiag, P.; Robert, C.; Grob, J.J.; Flaherty, K.T.; Arance, A.; Chiarion-Sileni, V.; Thomas, L.; Lesimple, T.; Mortier, L.; et al. Dabrafenib plus trametinib in patients with BRAF(V600)-mutant melanoma brain metastases (COMBI-MB): A multicentre, multicohort, open-label, phase 2 trial. *Lancet Oncol.* **2017**, *18*, 863–873. [[CrossRef](#)]
36. Long, G.V.; Trefzer, U.; Davies, M.A.; Kefford, R.F.; Ascierto, P.A.; Chapman, P.B.; Puzanov, I.; Hauschild, A.; Robert, C.; Algazi, A.; et al. Dabrafenib in patients with Val600Glu or Val600Lys BRAF-mutant melanoma metastatic to the brain (BREAK-MB): A multicentre, open-label, phase 2 trial. *Lancet Oncol.* **2012**, *13*, 1087–1095. [[CrossRef](#)]
37. Tawbi, H.A.; Forsyth, P.A.; Algazi, A.; Hamid, O.; Hodi, F.S.; Moschos, S.J.; Khushalani, N.I.; Lewis, K.; Lao, C.D.; Postow, M.A.; et al. Combined nivolumab and ipilimumab in melanoma metastatic to the brain. *N. Engl. J. Med.* **2018**, *379*, 722–730. [[CrossRef](#)]
38. Alexandrov, L.B.; Nik-Zainal, S.; Wedge, D.C.; Aparicio, S.A.; Behjati, S.; Biankin, A.V.; Bignell, G.R.; Bolli, N.; Borg, A.; Borresen-Dale, A.L.; et al. Signatures of mutational processes in human cancer. *Nature* **2013**, *500*, 415–421. [[CrossRef](#)]
39. Calapre, L.; Warburton, L.; Millward, M.; Ziman, M.; Gray, E.S. Circulating tumour DNA (ctDNA) as a liquid biopsy for melanoma. *Cancer Lett.* **2017**, *404*, 62–69. [[CrossRef](#)]
40. Johnson, D.B.; Menzies, A.M.; Zimmer, L.; Eroglu, Z.; Ye, F.; Zhao, S.; Rizos, H.; Sucker, A.; Scolyer, R.A.; Gutzmer, R.; et al. Acquired BRAF inhibitor resistance: A multicenter meta-analysis of the spectrum and frequencies, clinical behaviour, and phenotypic associations of resistance mechanisms. *Eur. J. Cancer* **2015**, *51*, 2792–2799. [[CrossRef](#)]
41. Long, G.V.; Fung, C.; Menzies, A.M.; Pupo, G.M.; Carlino, M.S.; Hyman, J.; Shahheydari, H.; Tembe, V.; Thompson, J.F.; Saw, R.P.; et al. Increased MAPK reactivation in early resistance to dabrafenib/trametinib combination therapy of BRAF-mutant metastatic melanoma. *Nat. Commun.* **2014**, *5*, 5694. [[CrossRef](#)]
42. Diefenbach, R.J.; Lee, J.H.; Rizos, H. Monitoring melanoma using circulating free DNA. *Am. J. Clin. Dermatol.* **2019**, *20*, 1–12. [[CrossRef](#)] [[PubMed](#)]
43. Calapre, L.; Giardina, T.; Robinson, C.; Reid, A.L.; Al-Ogaili, Z.; Pereira, M.R.; McEvoy, A.C.; Warburton, L.; Hayward, N.K.; Khattak, M.A.; et al. Locus-specific concordance of genomic alterations between tissue and plasma circulating tumor DNA in metastatic melanoma. *Mol. Oncol.* **2019**, *13*, 171–184. [[CrossRef](#)] [[PubMed](#)]
44. Hayward, N.K.; Wilmott, J.S.; Waddell, N.; Johansson, P.A.; Field, M.A.; Nones, K.; Patch, A.M.; Kakavand, H.; Alexandrov, L.B.; Burke, H.; et al. Whole-genome landscapes of major melanoma subtypes. *Nature* **2017**, *545*, 175–180. [[CrossRef](#)] [[PubMed](#)]
45. Li, H.; Durbin, R. Fast and accurate short read alignment with Burrows-Wheeler transform. *Bioinformatics* **2009**, *25*, 1754–1760. [[CrossRef](#)]
46. Li, H.; Handsaker, B.; Wysoker, A.; Fennell, T.; Ruan, J.; Homer, N.; Marth, G.; Abecasis, G.; Durbin, R.; Genome Project Data Processing, S. The sequence alignment/map format and SAMtools. *Bioinformatics* **2009**, *25*, 2078–2079. [[CrossRef](#)]

47. Sherry, S.T.; Ward, M.H.; Kholodov, M.; Baker, J.; Phan, L.; Smigielski, E.M.; Sirotkin, K. dbSNP: The NCBI database of genetic variation. *Nucleic Acids Res.* **2001**, *29*, 308–311. [[CrossRef](#)]
48. Genomes Project, C.; Auton, A.; Brooks, L.D.; Durbin, R.M.; Garrison, E.P.; Kang, H.M.; Korbel, J.O.; Marchini, J.L.; McCarthy, S.; McVean, G.A.; et al. A global reference for human genetic variation. *Nature* **2015**, *526*, 68–74. [[CrossRef](#)]
49. Sukhai, M.A.; Misyura, M.; Thomas, M.; Garg, S.; Zhang, T.; Stickle, N.; Virtanen, C.; Bedard, P.L.; Siu, L.L.; Smets, T.; et al. Somatic tumor variant filtration strategies to optimize tumor-only molecular profiling using targeted next-generation sequencing panels. *J. Mol. Diagn.* **2019**, *21*, 261–273. [[CrossRef](#)]
50. Fu, W.; O'Connor, T.D.; Jun, G.; Kang, H.M.; Abecasis, G.; Leal, S.M.; Gabriel, S.; Rieder, M.J.; Altshuler, D.; Shendure, J.; et al. Analysis of 6,515 exomes reveals the recent origin of most human protein-coding variants. *Nature* **2013**, *493*, 216–220. [[CrossRef](#)]
51. Lek, M.; Karczewski, K.J.; Minikel, E.V.; Samocha, K.E.; Banks, E.; Fennell, T.; O'Donnell-Luria, A.H.; Ware, J.S.; Hill, A.J.; Cummings, B.B.; et al. Analysis of protein-coding genetic variation in 60,706 humans. *Nature* **2016**, *536*, 285–291. [[CrossRef](#)]



© 2019 by the authors. Licensee MDPI, Basel, Switzerland. This article is an open access article distributed under the terms and conditions of the Creative Commons Attribution (CC BY) license (<http://creativecommons.org/licenses/by/4.0/>).